Int J Earth Sci (Geol Rundsch) (2007) 96:289–302
DOI 10.1007/s00531-006-0095-5

ORIGINAL PAPER

Integrated 3D density modelling and segmentation of the Dead Sea Transform

H.-J. Götze · R. El-Kelani · S. Schmidt · M. Rybakov · M. Hassouneh · H.-J. Förster · J. Ebbing

Received: 6 May 2005 / Accepted: 20 March 2006 / Published online: 31 May 2006

Abstract A 3D interpretation of the newly compiled Bouguer anomaly in the area of the ''Dead Sea Rift'' is presented. A high-resolution 3D model constrained with the seismic results reveals the crustal thickness and density distribution beneath the Arava/Araba Valley (AV), the region between the Dead Sea and the Gulf of Aqaba/Elat. The Bouguer anomalies along the axial portion of the AV, as deduced from the modelling results, are mainly caused by deep-seated sedimentary basins ($D > 10$ km). An inferred zone of intrusion coincides with the maximum gravity anomaly on the eastern flank of the AV. The intrusion is displaced at different sectors along the NNW–SSE direction. The zone of maximum crustal thinning (depth 30 km) is attained in the western sector at the Mediterranean. The southeastern plateau, on the other hand, shows by far the largest crustal thickness of the region (38–42 km). Linked to the left lateral movement of approx. 105 km at the boundary between the African and Arabian plate, and constrained with recent seismic data, a small asymmetric topography of the Moho beneath the Dead Sea Transform (DST) was modelled. The thickness and density of the crust suggest that the AV is underlain by continental crust. The deep basins, the relatively large intrusion and the asymmetric topography of the Moho lead to the conclusion that a small-scale asthenospheric upwelling could be responsible for the thinning of the crust and subsequent creation of the Dead Sea basin during the left lateral movement. A clear segmentation along the strike of the DST was obtained by curvature analysis: the northern part in the neighbourhood of the Dead Sea is characterised by high curvature of the residual gravity field. Flexural rigidity calculations result in very low values of effective elastic lithospheric thickness ($t_e < 5$ km). This points to decoupling of crust in the Dead Sea area. In the central, AV the curvature is less pronounced and t_e increases to approximately 10 km. Curvature is high again in the southernmost part near the Aqaba region. Solutions of Euler deconvolution were visualised together with modelled density bodies and fit very well into the density model structures.

Keywords Bouguer anomaly · 3D-density modelling · Flexural rigidity · Euler deconvolution · Dead Sea Transform

H.-J. Götze (✉) · S. Schmidt
Institut für Geowissenschaften, Abtlg. Geophysik,
Christian-Albrechts-Universität zu Kiel,
Otto-Hahn-Platz 1, 24118 Kiel, Gemany
e-mail: hajo@geophysik.uni-kiel.de

R. El-Kelani
An-Najah University, Nablus, Palestine

M. Rybakov
Geophysical Institute of Israel, Holon, Israel

M. Hassouneh
Natural Resources Authority, Amman, Jordan

H.-J. Förster
GeoForschungsZentrum, Potsdam, Germany

J. Ebbing
Norges Geologiske Undersøkelse,
7491 Trondheim, Norway

Introduction

The unique geological setting of the Dead Sea Transform (DST) makes this region a main focus of

interest for geoscientific research. The nature of the crust underlying the shoulders east and west of the Arava/Araba valley (AV) as well as the Dead Sea depression have been controversial among researchers for the past five decades. Consequently, the crustal structure of the AV and its eastern and western plateaus have been well studied and documented (Ginzburg et al. 1979a, b; Garfunkel 1981; Makris et al. 1983; Garfunkel and Derin 1984; El-Isa et al. 1987; Rotstein et al. 1987; Atallah 1992; Amiran et al. 1994; Frieslander 2000; Klinger et al. 2000; Ben-Avraham et al. 2002). Based on both reflection/refraction seismic experiments (Fig. 1) and gravity data, a gradual transition from the continental crust of the eastern part of the rift (Arabian Plate) with thicknesses of 35–40 km (El-Isa et al. 1987; Makris et al. 1983; Al-Zoubi and Ben-Avraham 2002) to the crust of the eastern Mediterranean (Palestine Sinai Plate) is interpreted. Here the crust is assumed to be partly underlain by typical oceanic crust with thicknesses smaller than 10 km (Ginzburg et al. 1979a; Makris et al. 1983; Ben-Avraham et al. 2002).

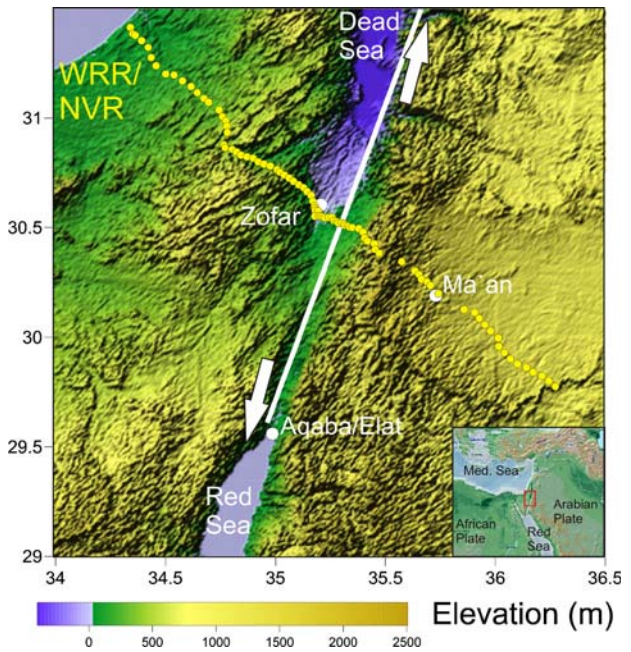

Fig. 1 Location map of the study area and the seismic experiments in the Middle East. The 260 km long wide-angle reflection/refraction profile (*WRR yellow circles*) crosses Palestine, Israel and Jordan. The near-vertical seismic reflection profile (*NVR*) coincides with the inner 100 km of the *WRR*. A *white line* indicates the Dead Sea Transform (DST) between the Dead Sea and the Red Sea. The *white arrows* indicate the left-lateral motion of 105 km between the African and Arabian plates in the last 20 My. *Background colours* show topography (gtopo30). The *inset* shows the regional features of the suture zone

Major components of the investigations under the framework of the international DESERT group (DESERT Group 2000, 2004) were combined reflection/refraction surveys across the territories of Palestine, Israel and Jordan, crossing the DST in the Arava/Araba Valley, where the geometry of the DST appeared to be relatively simple. The main seismic results can be described as: (1) the seismic basement is offset by 3–5 km below the DST, (2) the DST cuts through the entire crust, broadening in the lower crust, (3) strong lower crustal reflectors are only imaged on one side of the DST, (4) the seismic velocity sections show a steady increase in the depth of the crust–mantle transition (Moho) from ~26 km at the Mediterranean to ~39 km under the Jordan highlands, with only a small but visible, asymmetric topography of the Moho under the DST. These observations can be linked to the left-lateral movement of 105 km of the two plates, accompanied by strong deformation within a narrow zone cutting through the entire crust. Comparing the DST and the San Andreas Fault system (SAF), a strong asymmetry in sub-horizontal lower crustal reflectors and a deep reaching deformation zone both occur around the DST and the SAF. This suggests that these structures are fundamental features of large transform plate boundaries (DESERT Group 2004; Haberland et al. 2003; Maercklin et al. 2004; Sobolev et al. 2005; Mohsen et al. 2004).

A combination of seismic and magnetotelluric experiments showed, that a strong contrast across the Arava fault (AF, the name of the DST between the Dead Sea and the Gulf of Aqaba/Elat) exists; low seismic velocities and electric resistivities to the east and high seismic velocities and resistivities to the west (Ritter et al. 2003). It is therefore suggested that the reflector imaged by Maercklin et al. (2004) is the boundary between two blocks, offset from the present day location of the DST at the surface, which also acts as an impermeable seal isolating the two blocks over at least several hundred-thousand years (Maercklin et al. 2004). This is in marked contrast to findings at the San Andreas Fault. On an even smaller scale the analysis of fault-zone guided waves in the DST provided evidence for an extremely narrow region of reduced velocities (few meters) (Haberland et al. 2003), indicative of a near surface damage zone of the AF. This narrow occurrence could point towards the fact that absolute motion on the AF is much smaller than on the SAF, which has larger offsets and a thicker fault zone. On a larger, plate tectonic scale, Rümpker et al. (2003) were able to demonstrate that a distinct narrow vertical zone in the crust exists under the AF, where the Arabian and

the African plate are decoupled. This vertical zone even extends through the entire lithosphere.

In the present work, a 3D gravity model of the southern part of an area is presented, which is centred around the DST, and complement the existing interpretations of seismic surveys. The results of the DESERT seismic reflection/refraction experiments in the AV, which cross the eastern and western Jordan Rift Plateaus, have been used to constrain the initial 3D density model of both the DST and adjacent areas. The gravity database stems mainly from datasets of the Natural Resources Authority (NRA) of Jordan and the Geophysical Institute of Israel (GII) and was reprocessed and homogenised in the framework of the PhD thesis of Hassouneh (2003). In addition, the present study incorporates gravity data, which were collected and processed by joint collaboration of the DESERT Group from Germany (FU Berlin); Jordan (NRA); Israel (GII) and Palestine (An-Najah University).

Geological setting

General information from geology and tectonics of the study area has been incorporated both in the qualitative and quantitative interpretation stage of the observed Bouguer gravity anomaly. The geological maps of Jordan and Israel, compiled by the Natural Resources Authority of Jordan and the Geological Survey of Israel, were used to constrain the model at the surface. Due to ambiguities in potential field data interpretation a rather comprehensive knowledge of the regional geology of the AV and the adjoining region is necessary to constrain the model structures and interpretation of the gravity data in particular. In the following, a short introduction of the regional geology of the AV is given.

The DST is a system of left-lateral strike-slip faults that accommodate the relative motion between the African and Arabian plates. Except for a mild compressional deformation starting about 80 Ma ago, the larger Dead Sea region has remained a stable platform since the early Mesozoic. Approximately 17 Ma ago, this tectonic stability was interrupted by the formation of the DST, with a total left-lateral displacement of 105 km until today (Quennell 1958; Freund et al. 1970; Garfunkel 1981). The AV forms a part of the large Tertiary–Quaternary rift system which extends from the Gulf of Aqaba in the south to Syria and Turkey in the north (Fig. 1). The rift, like the rest of the East African Rift System, has undergone a very complicated geological evolution and tectonic history. The regional geology and structural evolution of the AV System have been extensively described and well documented (Quennell 1958, 1959, 1983; Bender 1974; Jarrar et al. 1983; Atallah 1992).

The pre-Cambrian basement rocks in the Dead Sea Rift System, except in the northern Aqaba/Elat gulf at the extreme south of the AV, are mostly covered by an (1) Early Cambrian volcanic sedimentary succession, (2) Mesozoic sediments and (3) more recent Tertiary volcanic rocks. The oldest sedimentary sequence, on the other hand, is masked by sediments of Middle to Upper Pleistocene age. In the rift valley thin deposits of Pleistocene–Holocene age are common. Late Paleozoic igneous rocks, early Cambrian volcano-sedimentary successions, and minor Cenocoic mafic volcanic rocks form the plateau adjoining the DST (Jarrar 1985).

The main trend of the tectonic structure in the Arava/Araba valley is the same as that of the AF, which is dominantly of NNE–SSW direction (Atallah and Mikbel 1983; Atallah 1992). Within the valley floor, three major geotectonical provinces are recognizable between latitudes 28° 00′ and 33° 20′: The Gulf of Aqaba/Elat, the Wadi Araba and the Dead Sea-northern region.

Recent geological and geochemical studies of the AF by the DESERT team show that now exhumed fault sections were deformed at temperatures between 150 and 300°C, indicating depths of up to 3 km. Analysis of the fluids in the fault shows that expulsed fluids were replaced by fluids from stratigraphically higher reservoirs on very short time scales and that the age of the AF is younger than 30 Ma (Janssen et al. 2004).

This brief summary shows that the Dead Sea region provides an excellent site to study geodynamic processes on different scales. This then facilitates an understanding of how the interplay of structure and dynamics controls the occurrence and rate of earthquakes. In this context an important aspect is that the DST crosses a land area, which was a stable platform throughout most of the Phanerozoic (Garfunkel 1981). Therefore, late Cenozoic activities can be observed in ‘‘pure form’’, without being masked by earlier events. Thus, the Dead Sea area is a unique natural laboratory. It allows the study of the geometry of upper crustal faulting, the mechanics of the lithosphere, and growth and subsidence of pull-apart basins. This pull-apart formation forms the most negative topographic feature on Earth. The Dead Sea lies approximately –430 m below normal sea level.

Gravity data

As described in the introduction, the international DESERT project was aimed at the investigation of the lithosphere at different scales in time and space. Therefore, it provides insight into differently scaled processes, which act on the transform. Towards this end, the gravity group worked on density models of the area at both, a regional and a local scale. To test the modelled gravity against the measured gravity field the first task was to homogenise existing databases (e.g. Hassouneh 2003). Gaps in the data coverage existed in particular in the central part of the DESERT project, where the seismic profile crosses the Arava fault and on the plateau in the south east (see Fig. 1).

The existing measurements were reprocessed by Hassouneh (2003), who calculated a topographic correction for the entire region and identified and corrected errors in the various databases. Unfortunately, only a few metadata (information about field campaigns, gravity meters, processing procedures) were available for this task. In many cases, data had to be eliminated, where no correction of the errors was possible (false station heights, geographic coordinates, gravity values, misprints and many other error sources). This modified data set was the basis of our studies—without further evaluation for consistency. In the Arava valley, the DESERT gravity team completed the database with additional measurements (refer to next chapter), to enable a more local gravity interpretation.

DESERT gravity campaign

From March to May 2002 the gravity survey was performed in the area of Sde-Boker and Zofar, with a general gravity station spacing of about 500 m. Detailed gravity measurements, with a station spacing of approx. 50 m, have been carried out in the Zofar area along the seismic lines GP-2150 and GP-2152 (Frieslander 2000). Some 480 gravity stations were measured at an average production rate of 50 stations per day. The gravity field data were collected using a Scintrex CG-3M AutoGrav gravity meter no. 808426. This instrument can measure variations in the Earth's gravity with a readout resolution of 0.01×10^{-5} m/s^2. The local survey west of the DST was linked via the Sde-Boker and E'n-Yahav base stations to Jordan's national gravity work (IGSN 72). Observations at these base stations were twice a day, in the morning and evening of each working day. During the field survey, the daily drift was less than 0.07×10^{-5} m/s^2 for the Scintrex meter. Repeated observations were carried out at all stations and resulted in an error of $\pm\ 0.02 \times 10^{-5}$ m/s^2. For height determinations of field stations, two Trimble GPS 5700 instruments were used in a real-time kinematics mode. Elevations were surveyed to the top of the instrument in real time with an accuracy of a few centimetres. All data were processed after the return from the field survey on the same day by the in-house JAVA software. Therefore, erroneous measurements could be detected instantly and occasionally remeasured.

Bouguer anomaly and isostatic residual gravity field

The DESERT Bouguer anomaly compilation integrates the following data sets:

- Regional gravity data by the Natural Resources Authority (NRA) of Jordan (Hassouneh, 2003).
- Regional gravity data by the Geophysical Institute of Israel (GII) (Rybakov, personal communication).
- The local DESERT gravity surveys of Sde-Boker and Zofar as described above.

In total we homogenised approximately 86,800 stations, covering the AV and the Dead Sea area. They are fairly uniformly spaced with an average distance of some 500 m. All stations are processed according to standard procedures, using the 1967 Geodetic Reference System and the standard density of 2.67 Mg/m^3. The terrain corrections were calculated up to Hayford zone O_2 (167 km), using a digital terrain model with a 25 m grid compiled by the Geological Survey of Israel (J.K. Hall, personal communication). The overall accuracy of the station complete Bouguer anomaly values are estimated to be 0.1×10^{-5} m/s^2. Figure 2 shows the central area of the derived Bouguer anomaly map with a constant contour interval of 5×10^{-5} m/s^2, based on a grid with 500 m node spacing. All anomalies range from 30×10^{-5} m/s^2 (maximum) to -120×10^{-5} m/s^2 (minimum). The highest Bouguer gravity values are located west of the AV; here the anomalies show a SW–NE trend. Due to the lack of meta data we cannot calculate an overall error of the Bouguer anomaly.

To enhance the local anomalies, which are caused by near surface density inhomogeneities, an isostatic regional gravity field has been calculated, based on the assumption of regional compensation, i.e. a Vening–Meinez model. The model parameters are:

Density of the topographical masses: 2.67 Mg/m^3
Density of the upper mantle: 3.3 Mg/m^3
Depth of the normal crust: 30 km
Flexural rigidity: 10^{23} N m

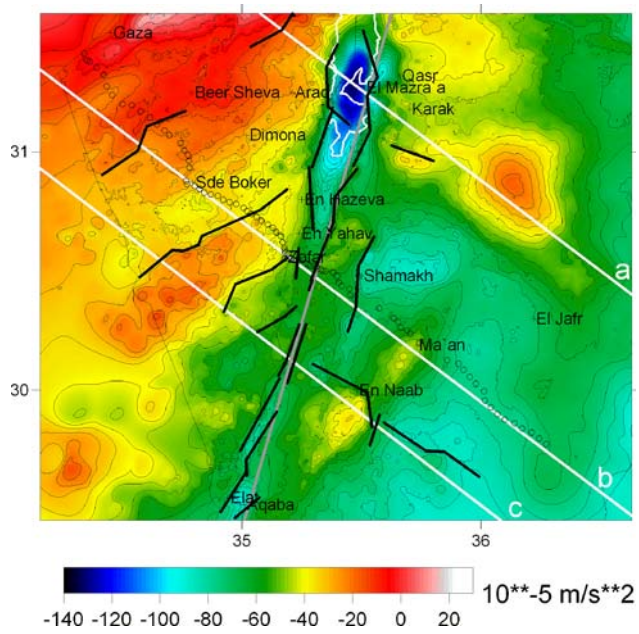

Fig. 2 The measured (complete) Bouguer anomaly map in the Dead Sea area (contour interval 5×10^{-5} m/s^2). The *white lines* mark the positions of the vertical cross-sections shown in Fig. 5 (cross-section *a* corresponds with Fig. 5a, *b* with Fig. 5b and *c* with Fig. 5c; the *grey line* indicates the vertical NS cross-section in Fig. 6. The *WRR* profile is indicated by *circles*

After subtracting this isostatic Vening Meinesz regional field from the Bouguer gravity field, we derived an ''isostatic residual field'', which is shown in Fig. 3. For further enhancement of local features in the isostatic residual gravity, we calculated the curvature of the field by another in-house software, based on algorithms published by Roberts (2001) (Fig. 4). Curvature is an attribute of a curve or a surface in the 2-D or 3D space, respectively, and describes, how much the curve deviates from a straight line (planar surface) and how bent a curve/surface is at a particular point. Therefore, curvature is a surface-related attribute which provides insight into particular aspects or properties of a surface, which are otherwise difficult or not possible to observe. From the methodological point of view it is related to the second derivative of the surface. Curvature has previously been used in the analysis of 3D seismic surveys (Roberts 2001), but has also been tested and applied on gravity data (Tašárová 2004). Here, we used ''dip curvature'' which is calculated in the direction of the largest dip of the Bouguer gravity ''surface''. It enhances linear features (gravity lineaments) in the residual field and may help to identify general strike directions. Figure 4 shows the mapped ''dip curvature'' of the isostatic residual field shown in Fig. 3. An interpretation of the gravity field is given in the following section.

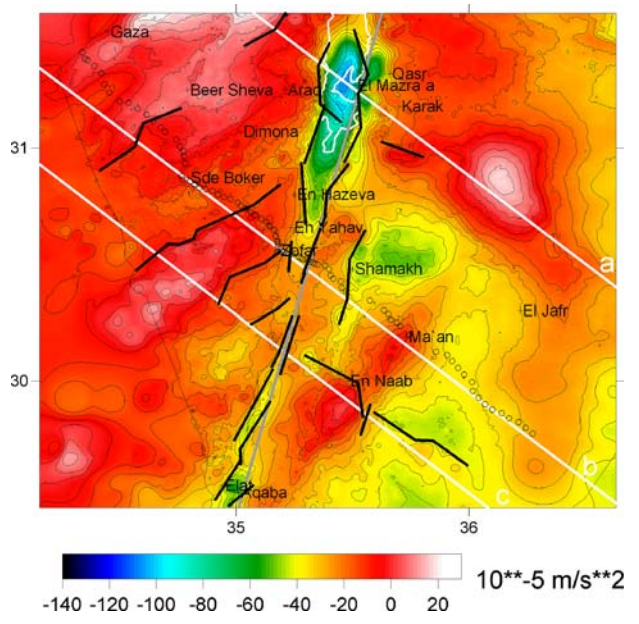

Fig. 3 Isostatic residual field, based on a Vening–Meinesz model (contour interval 5×10^{-5} m/s^2). The *WRR* profile is indicated by *circles*

Qualitative interpretation of resulting gravity fields

The Bouguer gravity anomalies (Fig. 2) do not show a unique trend. In general the magnitude of Bouguer

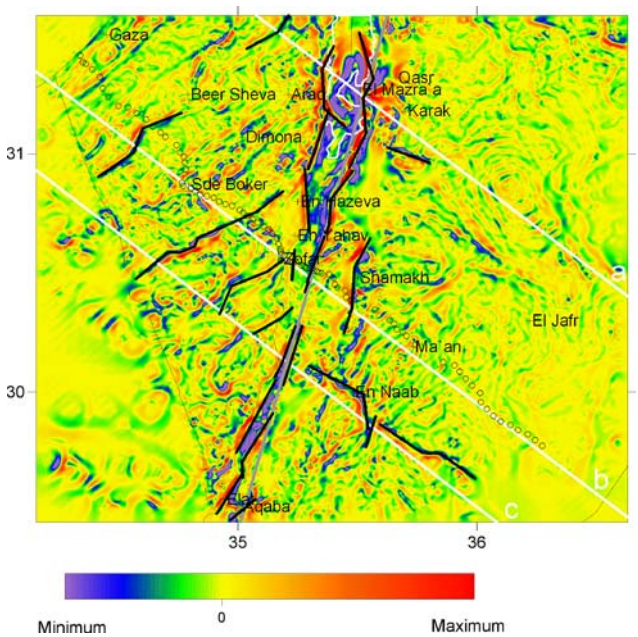

Fig. 4 Dip curvature of the isostatic residual field shown in Fig. 3. Negative curvatures are *blue*/*green* colours, while positive curvatures are shown in *orange*/*red* colours. Zero curvatures are *yellow*. The thick b*lack lines* represent an interpretation of some prominent curvature lineaments. *G* Gharandal basin, *T* Timna basin. The *WRR* profile is indicated by *circles*

anomaly remain on a rather low (negative) level, even close to the Mediterranean Sea barely reaches positive values. The anomalies indicate a thick crust, which increases from NW to SE. Due to a rather monotonous regional field the isostatic residual field shows similar features as the Bouguer gravity. In both, the Bouguer and isostatic anomalies (Fig. 2 and 3) the Dead Sea area is the most conspicuous feature in the map. The dominating feature is the extremely narrow gravity minimum of -130×10^{-5} m/s^2 which covers the Dead Sea region. This minimum extends to the south, decreasing up to the location of the DESERT profile and continues with an NNW–SSE offset of some 5 km further to the South. The same observation is made close to Aqaba/Elat, where again the pronounced minimum shows an offset of 5–10 km to the south-east. In addition, we observe here different gradients along both flanks of the valley: very steep in the east, and moderate along the western escarpment.

East of the DST there is a relatively dominant positive structure (-20×10^{-5} m/s^2 in the Bouguer field, Fig. 2), which was difficult to model (see also Results and discussion and Fig. 5a). Apart from this feature, the Bouguer gravity is characterised by values around –70 to -60×10^{-5} m/s^2 and approx. –20 to -25×10^{-5} m/s^2 in the isostatic residual field (Fig. 3). The maps reveal a relatively large-scale positive anomaly in the Jordan highlands (30.8° N, 36.1° E). This anomaly increases in an area of low topography and has its maximum of -10×10^{-5} m/s^2 along an axis of NNW–SSE trend. Closer geological and structural observation of the axis of the maximum anomaly suggests that its general trend follows an inferred zone of intrusions along the Karak-Wadi El-Fayha (KWF) fault system. This fault zone is related to a 1–2 km thick dyke system which extends from the Saudi-Arabian border to the Dead Sea region and can be seen in the geological map of Jordan (Bender 1975).

The different nature of the gravity (Figs. 2, 3) on the two opposite plateaus is marked by a steep gravity gradient along the eastern escarpment of the AV and a relatively moderate gravity gradient along the western escarpment. Apart from this anomaly the Bouguer gravity is characterised by values around –70 to -60×10^{-5} m/s^2 and therefore, the regional field was expected to be rather smooth. The residual gravity on the southeastern plateau reaches a minimum value of approx. -20×10^{-5} m/s^2 east of Ma'an (El-Jafr depression) whereas the residual gravity over the western plateau first decreases to values greater than 0×10^{-5} m/s^2 in the northwestern part, then gradually attains its maximum value of 20×10^{-5} m/s^2 in the north. The minimum anomaly in the AV is terminated at two places by NW–SE-trending gravity gradients.

In Fig. 4 some of the strongest values of gravity field curvature are highlighted by black lines. Curvature helps to segment the gravity field: east of the DST we calculated dominating SW–NE directions which are caused by the general strike of geological structures. The DST itself shows clear and strong dip curvature values in the north, but is weak in the central part where the seismic line crosses the fault system. In the central part the stronger dip curvature values jump to the east where they form a lineament passing the city of Shamakh. One may speculate that this lineament marks an active branch of the DST. Additional strong signals were obtained in the south close to Aqaba/Elat. Further to the north, stronger curvature values mark the edges of the young Gharandal and Timna basins (Fig. 4, G and T). In general the picture of dip curvature is more diffuse in the eastern part of the area than in the west and reflects the gravity anomalies caused by rather shallow seated density inhomogeneities in the crust.

Three-dimensional gravity modelling

Methodology and constraining data

As the Bouguer anomaly—apart from the elongated anomaly of the Dead Sea basin itself—shows highly irregular prominent features without any pronounced strike direction, 3D modelling, covering an area of approx. 240×270 km^2 was applied. The system used is the 3D forward gravity modelling package IGMAS (Interactive Gravity and Magnetic Application System), initially developed by Götze (1984); see also Götze and Lahmeyer (1988), and later modified towards a modern interpretation system (Schmidt and Götze 1999; Götze and Schmidt 2002). The kernel of the system essentially uses polyhedrons with triangulated surfaces to approximate bodies of constant density and/or susceptibility within the Earth's crust and mantle, the geometry of which is defined by a number of parallel vertical modelling sections. The position of the 14 vertical sections in the model used here, is chosen to be parallel to the seismic WRR/NVR profile (Fig. 1), i.e. roughly perpendicular to the DST. Fig. 2 contains only the location of those three cross-sections, which will be presented in Fig. 5. The distances between adjacent vertical sections are defined according to the requirements of the modelling of the observed Bouguer anomaly (Fig. 2).

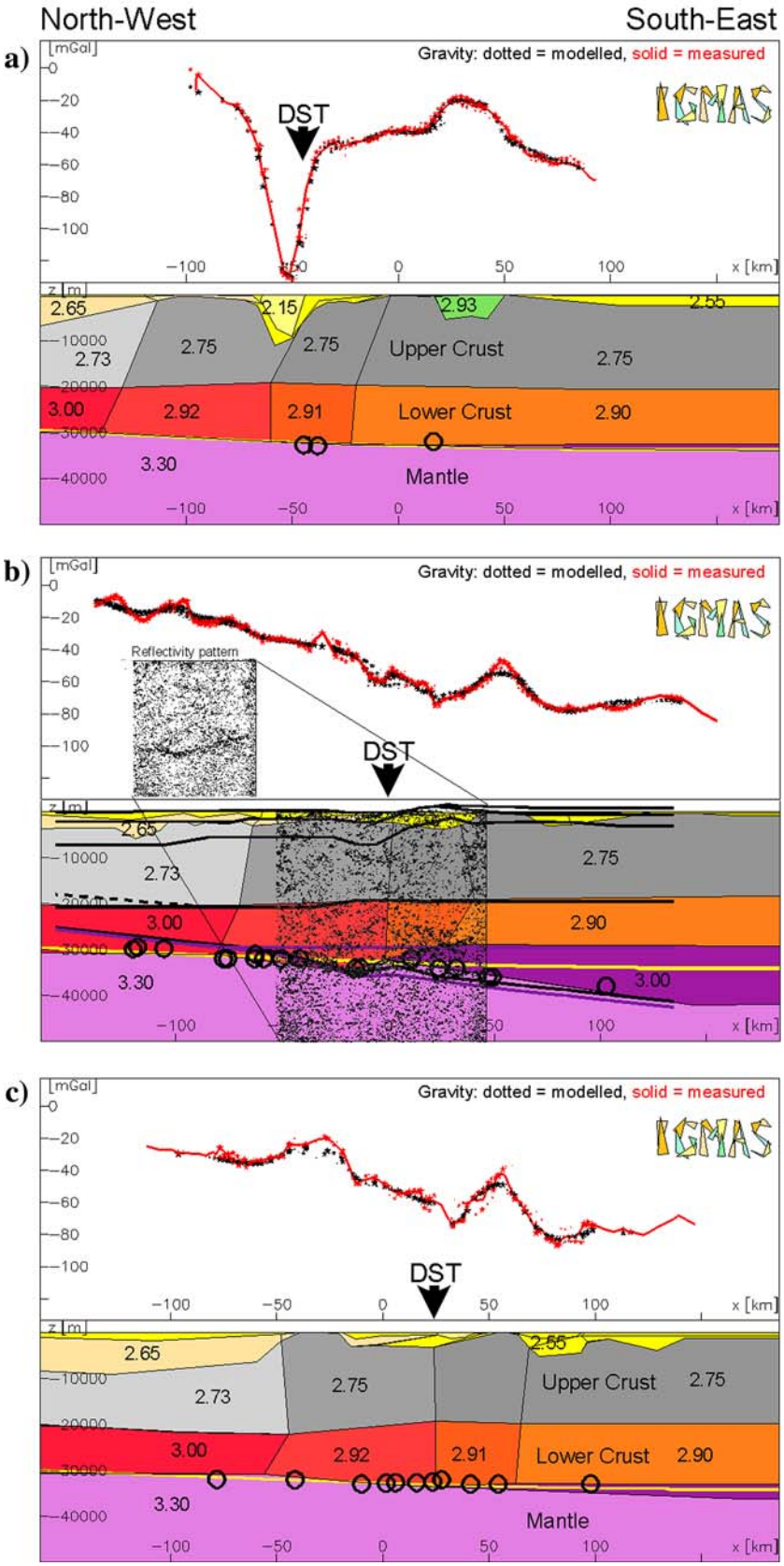

Fig. 5 Three vertical parallel cross-sections through the 3D density model (for location of profiles see Fig. 2). The distance between the cross-sections is approx. 60 km. The density values of the geologic units are given in Mg/m^3. The solid *black circles* indicate the Moho depth from the receiver function data (Mohsen et al. 2005). *DST* Location of the Dead Sea Transform fault. *Black overlay* NVR line drawing (DESERT group 2004), *black lines* indicate the interfaces of the seismic refraction model, *pink line* close to the Moho interface mark an alternative interpretation of the refraction seismic (DESERT group 2004). *Black dots* indicate the modelled gravity, the red line the measured gravity along the vertical cross-section

Constraints on geometry and densities

Modern interpretation of potential field data requires an interdisciplinary knowledge and integration to account for the "state of the art" information from comprehensive databases. This is why IGMAS provides GIS functions to integrate other geophysical models, information, and data from both geophysics and geology (Schmidt and Götze 1999; Breunig et al. 2000). The visualization of the additional information, which constrains the density modelling, can partly be seen in Figs. 5, 6 and 7. Several independent constraints were taken into account which stem from the other geophysical findings of the DESERT group:

- Geological observations constrain the most superficial structures.
- Reflection seismic helped to define the model geometry and refraction seismic velocities were converted into densities.
- The Moho position is supported by wide and steep angle seismics and receiver functions.
- Density determination in boreholes and petrophysical investigations have been used to fix the physical parameter density.
- Finally gravity studies on isostasy, Euler deconvolution, curvature and rigidity calculations help us to interpret the existing anomalies and sources of the observed gravity field in different parts of the gravity field spectrum.

The model benefited further from the knowledge of density distribution from top (surface) to bottom (Moho). Laboratory measurements include rocks from the uppermost sedimentary cover to the granulitic lower crust (H.-J. Förster, personal communication).

The upper crust in Jordan (with an average thickness of 20 km; El Isa et al. 1987; DESERT Group 2004; Mechie et al. 2005) is composed of sedimentary rocks of Cambrian to recent age overlying a Pan-African basement built up of igneous and metamorphic rocks of mostly late Proterozoic age (550–900 Ma). The Paleozoic portion of the sedimentary cover predominantly comprises quartz-rich sandstones and siltstones, with a minor contribution of mudstones and shales. This pile of rocks, which may reach a thickness of several kilometres, displays densities between 2.4 and 2.6 Mg/m^3. Measured densities for the Pan-African alkali feldspar granites, monzogranites, granodiorites, and orthogneisses are on the order of 2.57–2.65 Mg/m^3. Higher densities were obtained for Pan-African paragneisses and monzodiorites, which are in the range from 2.7 to 2.8 Mg/m^3. Important information on the composition of the lower crust and the upper mantle is provided by xenoliths entrained in Cenozoic basalts. Accordingly, two major groups of lower crustal rocks

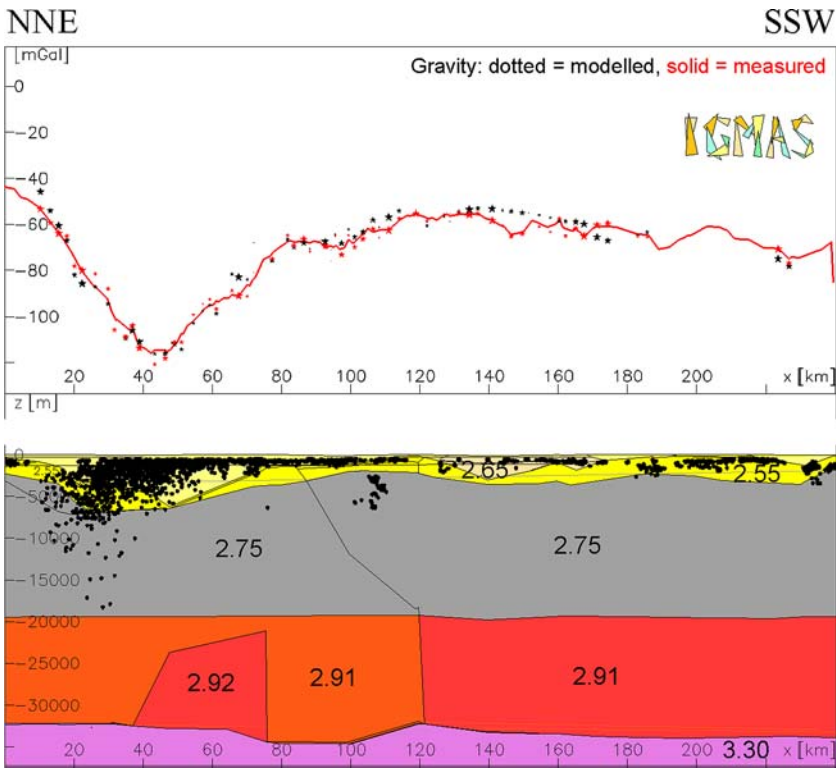

Fig. 6 North–South profile through the 3D model along the AV (for location of profile see Fig. 2). The *black points* show the position of the Euler deconvolution solutions (further explanation see text). The density values of the geologic units are given in Mg/m^3. *Black dots* indicate the modelled gravity, the *red line* the measured gravity along the vertical cross-section

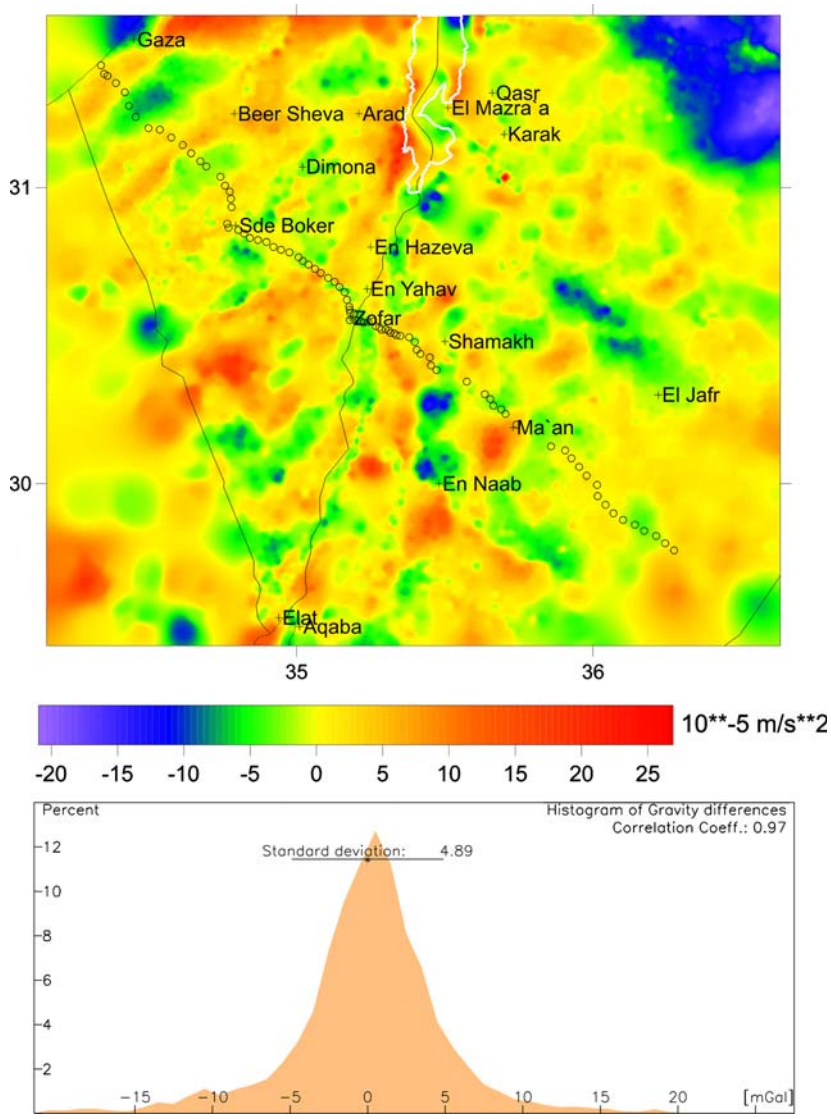

Fig. 7 Histogram of gravity differences (correlation coefficient 0.97). Also shown is the difference between the measured and modelled gravity anomaly. The SD of the gravity differences is 4.89×10^{-5} m/s^2. The *WRR* profile is indicated by *circles*

have to be distinguished: plagioclase-rich mafic granulites and two-pyroxene mafic granulites. Their relative abundance in the lower crust is well constrained from seismic P- and S-wave velocities (Mechie et al. 2005). Considering the recent *P–T* conditions of the lower crust, the values for V_p, V_s, and density (2.9–3.0 Mg/m^3) calculated from major-element composition of the plagioclase-rich granulites, using the approach of Sobolev and Babeyko (1994), are in good agreement with the seismic data. For the two-pyroxene granulites, densities of 3.05 Mg/m^3 and higher are implied. This density difference argues for a predominance of plagioclase-rich granulites in the lower crust of Jordan. The seismic data of El Isa et al. (1987) show local discontinuities at depths of about 30 km, which may reflect the presence of more denser rocks (i.e. two-pyroxene granulites) in the deeper portions of the lower crust to the Moho. The lithospheric mantle of Jordan and Israel is composed of peridotites, mostly harzburgites and lherzolites, for which a worldwide average of 3.3 Mg/m^3 is used in the gravity modelling.

The sources of constraining data pertaining to the geometry and density of the initial gravity model are various published and unpublished studies (Bender 1975; Haberland et al. 2003; Hassouneh 2003; Ritter et al. 2003; Rümpker et al. 2003; DESERT Group 2004; Kesten 2004; Maercklin 2004; Maercklin et al. 2004; Sobolev et al. 2005; Koulakov and Sobolev 2006; Mechie et al. 2005; Mohsen et al. 2005). In particular, the determination of the initial crustal thickness and density values for the deep structure of the rift are based on the results of the DESERT Project. The seismic reflection/refraction lines (near-vertical incidence reflection and wide-angle reflection/refraction

seismic) cross the western and eastern AV flanks in a NW–SE direction (DESERT Group 2004); results of receiver function analysis were taken from Mohsen et al. (2005). Table 1 shows the P-wave velocities of the structural units from the DESERT seismic experiment. Also shown are the estimated density values used for the regional 3D gravity modelling of the southern part of the AV.

Density measurements from several boreholes, drilled for geothermal investigations or oil exploration, have also been taken into consideration (Hassouneh, 2003; Hassouneh and Rybakov, personal communication). Although the boreholes are not deep enough to furnish density information on the deep crustal structure of the rift, the measured density values have been used to control the densities of the shallow rock units incorporated in the model.

Results and discussion

Due to the ambiguity of potential field interpretation the density model presented in this paper is one of several possible models, which has been developed by an iterative, interactive procedure, trying to satisfy as much constraining data as presently available.

Three parallel sections illustrate characteristic parts of the final density model (Fig. 5): the first section shows the model in its northern parts crossing the Dead Sea (Fig. 5a), the second (Fig. 5b) in the central sector of the AV was selected along the DESERT seismic line and a southern section (Fig. 5c) reflects the density structures in the south near Aqaba/Elat (see Fig. 2 for location of the sections). The model portrays crustal thicknesses and density distribution beneath the AV and its eastern and western rift flanks. It shows a steady increase in depth of the crust mantle transition (Moho) from ~29 km at the Mediterranean to ~42 km beneath the eastern plateau and confirms the asymmetric topography of the Moho beneath the DST (DESERT Group 2004; Mechie et al. 2005).

Table 1 The P-wave velocities of the geological units from the WRR seismic experiment

Geological units	Velocity Vp (km/s)	Density (Mg/m^3)
Sediments	3.3–5.2	2.50–2.65
Upper crust	6.1–6.2	2.70–2.75
Lower crust	6.7	2.90–3.00
Upper mantle	7.9	3.30

DESERT Group (2004) and corresponding densities

Model structures have densities of 2.15 Mg/m^3 for the valley deposits (Fig. 5), 2.55 Mg/m^3 for the Mesozoic carbonate platform, and 2.65 Mg/m^3 for Upper Cambrian/Lower Ordovician sandstones. A density of 2.72–2.75 Mg/m^3 was selected for the crystalline basement (Upper Crust), 2.9–3.0 Mg/m^3 for the Lower Crust and 3.3 Mg/m^3 for the upper mantle. The modelling showed that the regional NW–SE gravity trend is caused by the density contrast at the crust–mantle interface (Moho). The short-wavelength negative anomalies are effected by a sedimentary infill (Dead Sea depression, Gharandal and Timna basins, Fig. 4), and beneath the Ma'an plateau (El-Jafr depression). The short-wavelength positive anomalies were modelled by using densities of 2.72–2.75 Mg/m^3, which were assigned to different magmatic complexes in basement rocks at very shallow depths (0–0.2 km, in Fig. 5). The local residuals which remain between the measured and modelled fields shown above the cross-sections in Fig. 5, are best explained by near-surface mafic rocks that are located at different depths within the basement or sedimentary cover. They were not modelled because we are more interested in the regional density structures of the lithosphere. However, one of the intrusive structures was modelled (green body, Fig. 5a) by varying the geometry as well as its depth with a fixed density of 2.93 Mg/m^3. Tests showed, that the density of this hitherto unknown body could be set to 3.0 and even 3.1 Mg/m^3 by reducing the thickness of the structure. Normally such density points to mafic rocks from the lower crust and mantle. The modelled depth to the top of the intrusion ranges between 0.03 km and 0.32 km (below zero); its bottom, with an assigned density 2.93 Mg/m^3, is located within the crystalline basement at depths between 4.7 km and 5.5 km.

Gravity modelling has also to consider sediments of the AV and the Dead Sea depression. As discussed above, the negative anomalies are mainly caused by the low densities of the infill of local sediment basins. The lowest negative anomaly of approximately -130×10^{-5} m/s^2 in the Dead Sea area is well explained by a density value of 2.15 Mg/m^3 (Pleistocene sediment fills and salt). The total thickness of the Pleistocene sediments beneath the southern part of the Dead Sea depression, as obtained from the gravity modelling, amounts to more than 10 km. This value is in good agreement with results of 3D gravity modelling in the area of the central part of the Dead Sea basin, which indicates greater thicknesses of 12–16 km for Pleistocene sediments in the basin (Hassouneh 2003).

The crystalline basement (Figs. 5, 6), which is considered here to occur to a depth of approx. 20 km, has

been modelled by density values in the range of 2.72 Mg/m^3 beneath the western flank, and 2.75 Mg/m^3 beneath the eastern plateau. The top of the crystalline basement beneath the rift floor is generally marked by the maximum thickness of the sedimentary layer (more than 10 km). The crystalline basement has a thickness of ~9 km in the central sector of the AV. In general it thickens towards the adjoining plateaus (eastward and westward from the AV).

The centre of the gravity anomaly along the axial portion of the AV is well resolved. The gravity gradients, marking the two opposite facing escarpments of the rift, are also well modelled. The contour map of misfit between the measured and computed Bouguer anomalies of the study area (Fig. 7) reveals an average modelling discrepancy of $\pm 5 \times 10^{-5}$ m/s^2. However, for a regional gravity model, the computed Bouguer gravity map is acceptable.

Figure 6 presents a NNE–SSW section cutting through the 3D model along the axis of the AV, comparing the 3D model with the source solutions of an Euler deconvolution of the Bouguer gravity field. This combination of forward and inverse modelling techniques, shows clearly the segmentation along the DST. Euler deconvolution has been applied to potential field data for more than 30 years (e.g. Reid et al. 1990; Hoffmann 1999). It is based on Euler's homogeneity equation and helps to speed up interpretations of potential fields. Results are given as source points in space which indicate depths of bodies causing an anomaly (geological features). The solution depends on a structural index; here we used SI = –3 to approximate structures by mass points. To the north the Euler solutions point to masses at 5–8 km depth. They are concentrated in the basin and coincide with gradients in the gravity field and strong density contrasts. The majority of the Euler solutions are concentrated in the northern segment of the DST, below the Dead Sea basin. In the central part of the profile only a few solutions are present, indicating that there are mostly weak density contrasts in the upper crust. More to the south the number of source points increases again, although they remain at shallower depths (less than 5 km). This segmentation corresponds perfectly with the findings from dip curvature calculations which were presented in Fig. 4. It is assumed that the movements (activities) of the DST caused much higher density contrasts in the Dead Sea area due to massive and rapid sedimentation, than in the central part of the AV, where the seismic line crosses the DST. In the Aqaba/Elat region the fault system has again caused stronger density contrasts (and therefore higher gravity gradients) than in the central part.

The map of modelled Moho-depths shows another feature of regional importance. In Fig. 8, the modelled depths of the crust–mantle interface in coloured tones and results from receiver function analysis (Mohsen et al. 2005). The depth values from Mohsen et al. (2005) are calibrated by wide-angle seismic measurements (DESERT Group 2004). The receiver functions show, in good agreement with the density modelling, a depression of approx. 10–12 km. The crustal thickness distribution of the 3D model shows depths of 28–30 km in the northwest and a general dip down to approx. 35 km in the east and southeast. The AV separates the thinner crust in the NNW from thickened crust in the SSE. The trend in the Moho-depth map coincides well with the maximum gravity anomaly over the western flank of the rift, whereas the Moho depths correlate with the minimum gravity anomaly over the southeastern plateau. A new feature in the Moho depth map is the depression (D = 42 km) extending from the Ma'an area towards the southeast.

After applying curvature and Euler methods for a segmentation, there is a third method which provides insight into the nature of the DST. Fig. 9 shows the flexural rigidity expressed by the effective elastic thickness (T_e), which ranges from low (blue) to high values (red).

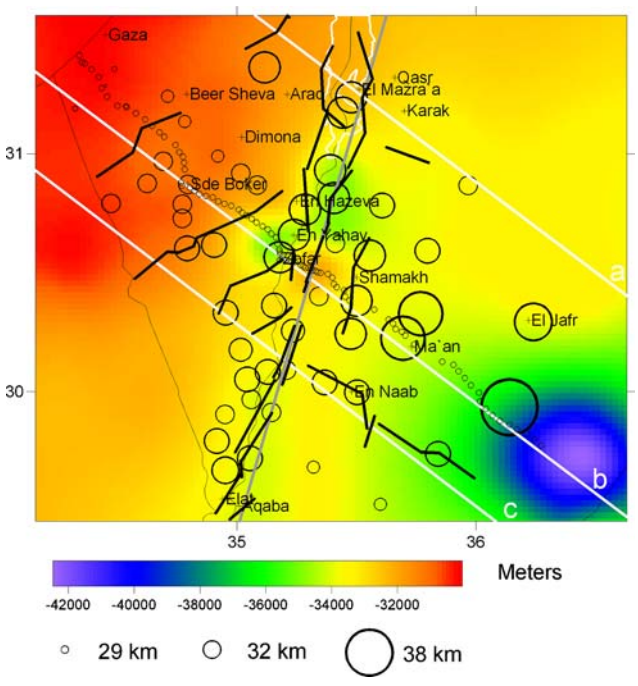

Fig. 8 Moho depth map beneath the 3D gravity modelling area of the Dead Sea. Also shown is the moho depth (*open circles*) from the receiver function data (Mohsen et al. 2005). The *WRR* profile is indicated by *circles*

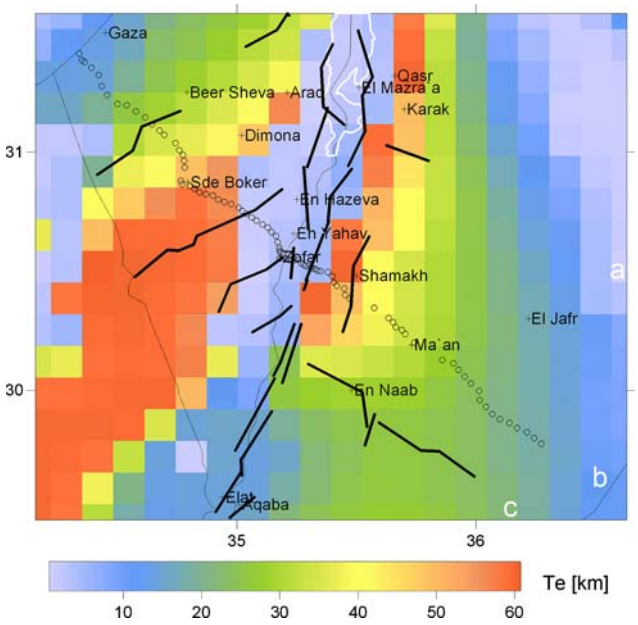

Fig. 9 Flexural rigidity map, derived by inversion of the topography using deconvolution. The scale shows the range of the T_e values in km. The *WRR* profile is indicated by *circles*

A relatively new scheme is used to estimate the flexural rigidity, or equivalently the elastic thickness of the lithosphere, given the topography and gravity data. The flexural rigidity is the parameter that governs the flexural response of the lithosphere in the frame of the thin plate flexure model. Our scheme is an alternative to the widely used calculation of admittance of topography (sea-floor or continental topography) and gravity (e.g. Watts 2001). The scheme involves the inversion of the gravity data in order to formulate a model of the Moho undulations. In a second step the flexure parameter is then evaluated from the relation between topography and Moho interface variations. Instead of calculating the admittance function using a spectral analysis, a set of point-load response functions are used in order to retrieve the optimal flexure parameter (the convolution method is described in, e.g. Braitenberg et al. 2002; Ebbing and Götze 2003; Ebbing 2004). This has two main advantages: instabilities of the numerical admittance evaluation at wave-numbers with low spectral energy in the topography are overcome and the analysis can be made over an area which is not necessarily rectangular, as required for the spectral analysis. The proposed method also allows a higher space resolution of elastic thickness than any spectral method.

Figure 9 presents a rather complicated picture of this lithospheric rigidity. West of the DST an area of rather high values of T_e = 60 km trends from southwest to northeast. At longitude 35° E it is replaced by a small area of intermediate rigidity and close to the AV in the area of DST by values close to 0 km. This zone is bordered by the gravity lineaments which were calculated by the curvature method (Fig. 4). South of the area where the DESERT seismic line crosses the DST, flexural rigidity increases again to intermediate values of T_e = 15 km in the Aqaba/Elat area. The eastern shoulder of the AV (the small area extending from En Naab via Shamakh to Karak) shows T_e values of 55 km which are similar to the ones of the western shoulder. More to the east, flexural rigidity drops down to smaller values, which will not be interpreted because we assume to see numerical artefacts due to boundary effects inherent to the method used. We consider the area with the high flexural rigidity to be the ''normal'' situation and the rigidity lows along the DST to be the interesting abnormal one. Burov and Diament (1996) state that in areas of decoupled crust and/or mantle, flexural rigidity is extremely low. The extreme gravity low in the northern segment (Dead Sea basin) and the strong gravity gradients here point to deep reaching disturbances of the crust and mantle system. One of the most significant results of the DESERT Group (2004) and Rümpker et al. (2003) was the finding that the DST cuts through the entire crust. Our analysis of the gravity field supports this finding. High temperatures (Sobolev et al. 2005) may additionally contribute to crust–mantle decoupling. However, if we accept that the northern segment is decoupled, the central and southern parts of the DST are not.

Conclusions

The new compilation of the DESERT Bouguer anomaly of the AV and adjacent areas was reinterpreted by (1) 3D density modelling using constraining data from other geophysical disciplines, including mainly the DESERT seismic experiments, (2) curvature analysis of the residual gravity field, (3) Euler deconvolution of the gravity field and, (4) studies of flexural rigidity of the lithosphere. These methods enabled us to establish a density model along the AV Transect (DESERT project). The seismic information and the uniform ground coverage of the gravity points helped in modelling and interpreting the gravity data which reveal some aspects about the crustal structure of the AV that are useful for supplementing other constrains in the geological synthesis. The gravity data are useful for delineating shallow and deep structures and help to define models in agreement with the basic information supplied by the geophysical investigations, as well as, from geological studies.

The Bouguer anomalies are caused by a combination of various sources located at different depths. The most prominent feature of the Bouguer map is the presence of a minimum anomaly in the rift floor which coincides with the boundary of the Dead Sea basin as a full-graben and reaches a minimum value of -130×10^{-5} m/s^2 over the northern part of the Dead Sea. The negative Bouguer gravity on the south eastern plateau reaches a minimum value of -80×10^{-5} m/s^2 east of Ma'an (El-Jafr depression), whereas the positive gravity anomaly over the western plateau attains a maximum value of 30×10^{-5} m/s^2 in the north and correlates with a high density value of the upper crust material beneath the north western part of the modelling area. A relatively large-scale local positive Bouguer anomaly occurs over the Jordanian highlands, with a maximum value of -20×10^{-5} m/s^2 along an axis of NW–SE trend. This general trends follows an inferred zone of intrusion along the Karak-Wadi El-Fayha (KWF) fault system.

The 3D gravity model is constrained by the information from the DESERT seismic experiments in the AV and points to the necessity of seismic studies through the Dead Sea. The final 3D gravity model indicates that the AV and its eastern and western plateaus are underlain by a continental crust with assigned densities ranging from 2.65 to 2.9 Mg/m^3. The negative Bouguer anomaly over the Dead Sea basin is modelled as caused by internal sedimentary basins filled with low-density, young sediments (2.15 Mg/m^3) and depths in the range of 8–12 km. The local positive anomaly SE of Karak, on the other hand, is modelled as differentiated basic igneous material (intrusion) within the uppermost part of the crust (<1 km) using the densities of 2.93, 3.0 and 3.1 Mg/m^3. This intrusion is most probably of mantle or crust–mantle origin.

The Moho-depth map indicates the thinning of the crust beneath the western flank of the rift to 30 km, and the thickest crust beneath the south eastern plateau (38–42 km). Beneath the DST, an asymmetric topography of the Moho is modelled.

Our study gives new insights into the crustal structure of the DST, which will help in future studies to determine the regional setting of the Arabian Peninsula.

Acknowledgments We wish to thank the DESERT Working Group at the GeoForschungsZentrum (GFZ) Potsdam for providing ''constraining data'' and their ongoing interest. In particular we are thankful to D. Kesten, N. Maercklin, J. Mechie, C. Haberland, A. Förster, S. Sobolev, N. Balling (reviewer) and an anonymous reviewer for useful discussions and suggestions, and especially M. Weber, the leader of the DESERT project, for many discussions and his valuable comments on an earlier version of this paper. Many thanks to J. Mechie for his careful language editing. R. El-Kelani and M. Rybakov would like to thank the Deutsche Forschungsgemeinschaft (DFG) and the GeoForschungsZentrum (GFZ) Potsdam for financing their sabbatical during this research. We are thankful to the Natural Resources Authority (NRA) of Jordan and the Geophysical Institute of Israel (GII) for providing their databases. The gravity research was funded by the Deutsche Forschungsgemeinschaft (DFG).

References

Al-Zoubi A, Ben-Avraham Z (2002) Structure of the earth's crust in Jordan from potential field data. Tectonophysics 346:45–59

Amiran DHK, Arieh E, Turcotte T (1994) Earthquakes in Israel and adjacent areas: macroseismic observations since 100 BCE. Israel Explor J 44:260–305

Atallah M (1992) Tectonic evolution of northern Wadi Araba, Jordan. Tectonophysics 204:17–26

Atallah M, Mikbel S (1983) Geology and structure of an area east of the Dead Sea. In: Abed AM, Khaled HM (eds) Proceeding the 1st Jordan Geol Conf, Sep 1982, Amman, 392–414

Bender F (1974) Geology of Jordan. Gebr Borntraeger, Stuttgart, pp 196

Bender F (1975) Geological map of Jordan, 1:500000. Government of Jordan and Geological Survey of the FRG

Ben-Avraham Z, Ginzburg A, Makris J, Eppelbaum L (2002) Crustal structure of the Levant Basin, eastern Mediterranean. Tectonophysics 346:23–43

Braitenberg C, Ebbing J, Götze H-J (2002) Inverse modeling of elastic thickness by convolution method—the Eastern Alps as a case example. Earth Planet Sci Lett 202:387–404

Breunig M, Cremers AB, Götze HJ, Schmidt S, Seidemann R, Shumilov S, Siehl A (2000) Geological mapping based on 3D models using an Interoperable GIS. Geo-Information-Systems, J Spat Inform Dec Making. 13: 12–18. ISSN 0935-1523

Burov EB, Diament M (1996) Isostasy, effective elastic thickness (EET) and inelastic rheology of continents and oceans. Geology 24:419–422

DESERT Group (2000) Multinational geoscientific research effort kicks off in the Middle East. EOS 81:609 616–617

DESERT Group (2004) The crustal structure of the Dead Sea Transform. Geophys J Int 156: 655–681

Ebbing J (2004) The crustal structure of the Eastern Alps from a combination of 3D gravity modelling and isostatic investigations. Tectonophysics 380(1–2): 80–104

Ebbing J and Götze HJ (2003) The collision of the European and Adriatic plates in the Eastern Alps—insights from 3D density modelling and isostatic investigations. In: TRANSALP Conference, Memorie di Scienze Geologiche, vol 54 (speciale), ISSN 0391-8602:37–41

El-Isa Z, Mechie J, Prodehl C, Makris J, Rihm R (1987) A crustal structure study of Jordan derived from seismic refraction data. Tectonophysics 138: 235–253

Freund R, Garfunkel Z, Zak I, Goldberg M, Weissbrod T, Derin B (1970) The shear along the Dead Sea rift. Philos Trans R Soc London 267:107–130

Frieslander U (2000) The structure of the Dead Sea Transform emphasizing the Arava, using new geophysical data. PhD Thesis, Hebrew University, Jerusalem, p 101

Garfunkel Z (1981) Internal structure of the Dead Sea leaky transform (rift) in relation to plate kinematics. Tectonophysics 80:81–108

Garfunkel Z, Derin B (1984) Permian-early Mesozoic tectonism and continental margin formation in Israel and its implications for the history of the Eastern Mediterranean. In: Dixon JE, Robertson AHF (eds) The geologic evolution of the eastern Mediterranean. Geol Soc Spec Pub, 187–201

Ginzburg A, Makris J, Fuchs K, Prodehl C, Kaminski W, Amitai U (1979a) A seismic study of the crust and upper mantle of the Jordan–Dead Sea Rift and their transition toward the Mediterranean Sea. J Geophys Res 84:1569–1582

Ginzburg A, Makris J, Fuchs K, Perathoner B, Prodehl C (1979b) Detailed structure of the crust and upper mantle along the Jordan–Dead Sea Rift. J Geophys Res 84:5605–5612

Götze HJ (1984) Über den Einsatz interaktiver Computergrafik in Rahmen 3-dimensionaler Interpretationstechniken in Gravimetrie und Magnetik. Habiltationsschrift, TU Clausthal, p 236

Götze HJ, Lahmeyer B (1988) Application of 3-D interactive modelling in gravity and magnetics. Geophysics 53:1096–1108

Götze HJ, Schmidt S (2002) Geophysical 3D Modeling using GIS-Functions. In: 8th annual conference of the international association for mathematical geology. Terra Nostra, pp 87–92. ISSN: 0946-8978

Haberland Ch, Agnon A, El-Kelani R, Maercklin N, Qabbani I, Rümpker G, Ryberg T, Scherbaum F, Weber M (2003) Modeling of seismic guided waves at the Dead Sea Transform. J Geophys Res 108(B7): 2342. DOI 10.1029/2002JB002309

Hassouneh M (2003) Interpretation of potential fields by modern data processing and 3-dimensional gravity modelling of the Dead Sea pull-apart basin/Jordan Rift Valley (JRV). Dissertation, Uni Würzburg, p 110

Hoffmann M (1999) Dreidimensionale Interpolation und Interpretation von Schwerefeldern. Diplomarbeit Institut für Geologie, Geophysik und Geoinformatik, FU Berlin, p 65

Janssen CH, Romer RL, Hoffmann-Rothe A, Kesten D, Al-Zubi H, DESERT Group (2004) The Dead Sea Transform: evidences for a strong fault? J Geol 112: 561–575

Jarrar GH (1985) Late Proterozoic evolution of the Arabian–Nubian Shield in the Wadi Araba area, southwest Jordan. Geologisches Jahrbuch Reihe 61:3–87

Jarrar GH, Baumann A, Wachendorf H (1983) Age determinations in the Precambrian basement of the Wadi Araba, southwest Jordan. Earth Planet Sci Lett 63:292–304

Kesten D (2004) Structural observations at the Southern Dead Sea Transform from seismic reflection data and ASTER satellite images. Dissertation, GFZ Potsdam, p 94

Klinger Y, Avouac JP, Dorbath L, Abou Karaki N, Tisnerat N (2000) Seismic behaviour of the Dead Sea fault along Araba Valley, Jordan. Geophys J Int 142:769–782

Koulakov I, Sobolev SV (2006) Moho depth and three-dimensional P and S structure of the crust and uppermost mantle in the Eastern Mediterranean and Middle East derived from tomographic inversion of local ISC data. Geophys J Int 164:218–235

Maercklin N (2004) Seismic structure of the Arava Fault, Dead Sea Transform. PhD Thesis, Scientific Technical Report STR04/12, GFZ Potsdam

Maercklin N, Haberland Ch, Ryberg T, Weber M, Bartov Y, DESERT Group (2004) Scattering of seismic waves at the Dead Sea Transform. Geophys J Int158(1):179–186

Makris J, Ben-Avraham Z, Behle A, Ginzburg A, Giese P, Steinmetz L, Whitmarsch RB, Eleftheriou S (1983) Seismic refraction profiles between Cyprus and Israel and their interpretation. Geophys J R Astr Soc 75:575–591

Mechie J, Abu-Ayyash K, Ben-Avraham Z, El-Kelani R, Mohsen A, Rümpker G, Saul J, Weber M (2005) Crustal shear velocity structure across the Dead Sea Transform from 2-D modelling of project DESERT explosion seismic data. Geophys J Int 160(3): 910–924. DOI 10.1111/j.1365-246X.2005.02526.x

Mohsen A, Hofstetter R, Bock G, Kind R, Weber M, Wylegalla K, DESERT Group (2005) A receiver function study across the Dead Sea Transform. Geophys J Int 160(3): 948–960. DOI 10.1111J.1365-246X.2005.02534.x

Quennell AM (1958) The structural and geomorphic evolution of the Dead Sea rift, Quart J Geol Soc London 114:2–24

Quennell AM (1959) Tectonic of the Dead Sea Rift. Cong Geol Int Mexico 22:385–405

Quennell AM (1983) Evolution of the Dead Sea RIFT. A review In: Abed AM, Khaled HM (eds) Proceedings 1st Jord Geol Conf, Amman 460–482

Reid AB, Allsop JM, Granser H, Millet AJ, Somerton IW (1990) Magnetic interpretation in three dimensions using Euler deconvolution. Geophysics 55:80–91

Ritter O, Ryberg T, Weckmann, U, Hoffmann-Rothe A, Abueladas A, Garfunkel Z, DESERT Group (2003) Geophysical images of the Dead Sea Transform in Jordan reveal an impermeable barrier for the fluid flow. Geophys Res Lett 30(14): 1741. DOI 10.1029/2003GL017541

Roberts A (2001) Curvature attributes and their application to 3D interpreted horizons. First break volume 19.2

Rotstein Y, Yuval Z, Trachtman P (1987) Deep seismic reflection studies in Israel—an update. Geophy J R astr Soc 89:389–394

Rümpker G, Ryberg T, Bock G, DESERT Seismology Group (2003) Boundary-layer mantle flow under the Dead Sea Transform fault from seismic anisotropy. Nature 425:497–501

Schmidt S, Götze HJ (1999) Integration of data constraints and potential field modelling—an example from Southern Lower Saxony, Germany. Physics and Chemistry of the Earth, Part A, 24(3): 191–196

Sobolev SV, Babeyko AYU (1994) Modelling of mineralogical composition, density and elastic wave velocities in anhydrous magmatic rocks. Surv Geophys 15:515–544

Sobolev SV, Petrunin A, Garfunkel Z, Babeyko AYU, DESERT Group (2005) Thermo-mechanical model of the Dead Sea Transform. Earth Planet Sci Lett 238:78–95

Tašárová Z (2004) Gravity data analysis and interdisciplinary 3D modelling of a convergent plate margin (Chile, 36E–42E). PhD Thesis, Freie Universität Berlin. http://www.diss.fu-berlin.de/2005/19/

Watts AB (2001) Isostasy and flexure of the lithosphere. Cambridge University Press, Cambridge, p 458